Temperature-Induced Micelle-Vesicle Transitions in DMPC−SDS and DMPC−DTAB Mixtures Studied by Calorimetry and Dynamic Light Scattering

Pinaki R. Majhi and Alfred Blume*

Institute of Physical Chemistry, Martin-Luther-Universitaet Halle-Wittenberg, Muehlpforte 1, D-06108 Halle/Saale, Germany

Received: March 28, 2002; In Final Form: June 27, 2002

The solubilization of dimyristoylphosphatidylcholine (DMPC) vesicles by the surfactant sodium dodecyl sulfate (SDS) or dodecyltrimethylammonium bromide (DTAB), respectively, was studied by isothermal titration calorimetry (ITC) at 30 and 60 °C and at different lipid concentrations. The partitioning of surfactant into lipid bilayers and the following solubilization of vesicles show a temperature dependence due to hydrophobic interactions, which is similar to temperature dependence of the cmc of surfactants. From the ITC data, we constructed phase diagrams in the total surfactant vs lipid concentration and surfactant concentration vs temperature plane, respectively. The micellar, the coexistence, and the vesicular region can not only be reached by concentration changes but also by simply raising the temperature of a lipid-surfactant mixture with a fixed concentration. From these phase diagrams, the transition temperature for a particular lipid−surfactant mixture can be predicted. The predictions were verified by following the temperature-induced formation of fluid vesicles from mixed micelles upon heating a lipid−surfactant mixture. The micelle−vesicle transitions of mixtures of DMPC with SDS or DTAB in water and the reverse transition to mixed micelles observed upon cooling was studied by differential scanning calorimetry (DSC), turbidity measurements using UV−vis spectrophotometry, and dynamic light scattering methods. The endothermic effects observed in the DSC curves for the micelle−vesicle transition are a consequence of the endothermic heats of transfer of surfactant as well as lipid from a mixed micelle to a mixed vesicle as determined by ITC.

Introduction

A large body of work has been performed concerning surfactant-induced solubilization of lipid vesicles which are used as model biomembrane systems.[1−4] The vesicle-to-micelle transformations induced by the incorporation of a surfactant into phospholipid vesicles are well studied,[5−10] but studies of the temperature-dependent behavior of mixed lipid−surfactant systems are rare.[11−15] The formation of lipid vesicles from surfactant/lipid mixed micelles, i.e., the micelle−vesicle transition, is based on surfactant removal from mixed micelles by dilution or dialysis.[5,16] The same result can be achieved by simply raising the temperature of a lipid/surfactant mixture of an appropriate composition.[12] Because of the simplicity of the temperature induced micelle−vesicle transition in lipid−surfactant mixtures, it can in principle be also used for the solubilization of membrane proteins by cooling a membrane saturated with surfactant, or the reconstitution of the membrane proteins into lipid vesicles by heating of mixed micelles.

Some reports have been published on the micelle−vesicle transition with an arbitrary concentration ratio of the lipid−surfactant mixture,[11−15] but in certain cases, this transition also involves a change of order of the lipids, i.e., the formation of mixed micelles with an ordered core,[11,13] and not the formation of fluid vesicles. Also, the complete phase diagram for a particular system has in general not been analyzed in detail, which is necessary for the prediction of the transition temperature and for the explanation of the transition pathway.

For the construction of this type of phase diagram, we have first studied the solubilization of lipid vesicles by adding surfactant to lipid vesicles using isothermal titration calorimetry (ITC). ITC is an ideal method to study the surfactant partitioning into lipid bilayers and surfactant-induced solubilization of lipid vesicles.[17−23] There are many reports on the construction of phase diagrams of the lipid−surfactant−water system in the framework of the three-stage model according to Lichtenberg[24−26] (Figure 1). According to this model, surfactants can be incorporated into the lipid vesicles up to a critical saturating surfactant/lipid ratio, R_e^{sat}, which describes the effective concentration of the surfactant in the bilayer in relation to the total lipid concentration. Beyond R_e^{sat}, the vesicles are destroyed and lipid saturated mixed micelles of a minimum effective surfactant/lipid ratio R_e^{sol} coexist with detergent saturated vesicles. When the total surfactant content in the aggregates reaches R_e^{sol}, all vesicles have disappeared and only mixed micelles exist indicating the complete solubilization.

Studies on the temperature effect on this type of phase behavior are rare. We studied the solubilization of DMPC vesicles by SDS and DTAB respectively at 30 and 60 °C and observed a characteristic change of the phase boundary lines. These shifts are caused by the "hydrophobic effect" and are similar to the change of the *cmc* of surfactants with temperature. From the ITC data taken at different temperatures, we constructed a phase diagram by plotting the total surfactant concentrations at the phase boundary lines vs temperature at a fixed lipid concentration. From this type of phase diagram, one can easily see that the micellar, coexistence, and finally vesicular state can be reached by using an appropriate mixture of lipid

* To whom correspondence should be addressed. Phone: +49-345-55-25850. Fax: +49-345-55-27157. E-mail: blume@chemie.uni-halle.de.

10.1021/jp025849b CCC: $22.00
Published on Web 09/19/2002

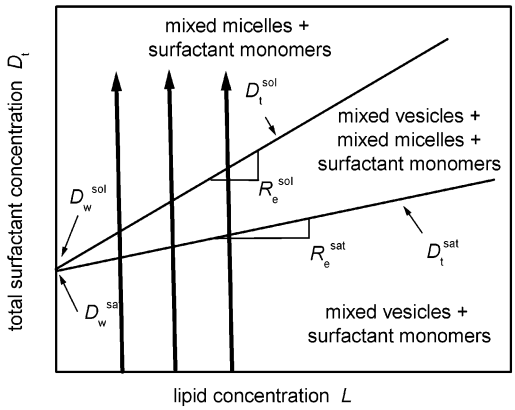

Figure 1. Scheme of a lipid−surfactant phase diagram in idealized form with the existence regions of micelles and vesicles. The arrow indicates the direction of the solubilization experiment in ITC. The total surfactant concentrations at the break points correspond to saturation and solubilization of the lipid vesicles, i.e., D_t^{sat} and D_t^{sol}, respectively, and D_w corresponds to the hypothetical critical aggregation concentration of the surfactant in the presence of lipid vesicles at zero concentration.

and surfactant and heating or cooling it over a certain temperature range. We have constructed these phase diagrams for the two different DMPC/surfactant systems and verified the micelle−vesicle transition by monitoring the change of heat capacity, turbidity, and particle size using differential scanning calorimetry (DSC), UV−visible spectrophotometry, and dynamic light scattering (DLS), respectively. The ITC data on the isothermal solubilization of vesicles by surfactants could be used to understand the endothermic effects observed upon heating and crossing the coexistence region of mixed micelle and mixed vesicles. These effects could be assigned to the endothermic heats of transfer of surfactant and lipid into the lipid vesicles.

Experimental Section

Materials. 1,2-Dimyristoyl-*sn*-glycero-3-phosphorylcholine (DMPC), sodium dodecyl sulfate (SDS), and dodecyltrimethylammonium bromide (DTAB) were products purchased from Sygena (Rheinfelden, Germany), Aldrich, Germany, and Merck, Germany, respectively. The products were used without further purification.

Preparation of Solutions. Surfactant solutions of a defined concentration were freshly prepared by weighing a certain amount of surfactant and dissolving it in deionized water. These solutions were used for the solubilization of lipid vesicles using ITC.

For the preparation of lipid vesicles, aqueous dispersions of the DMPC were first prepared by adding the appropriate amounts of lipid to deionized water and subsequent vortexing of the sample in a vial for 5 min at 40 °C. The coarse dispersions were then extruded (15 times each sample) at 40 °C through polycarbonate membranes to obtain unilamellar lipid vesicles of 100 nm diameter. These freshly prepared vesicle dispersions were then used directly for the solubilization experiment. For extrusion, the Liposofast extrusion device (Avestin, Canada) with polycarbonate membranes of 100 nm pore size was used.

For lipid−surfactant mixtures, concentrated solutions of surfactant and lipid were prepared separately, as mentioned above. These solutions were mixed using the desired molar ratio and then diluted with deionized water to the final concentration of components in the mixture.

ITC Measurements. ITC experiments were performed using a Microcal MCS isothermal titration calorimeter (Microcal, Inc., Northampton, MA). The removable integrated injection−stirrer syringe (250 μL) was filled with a concentrated solution of a surfactant which was added in multiple steps (5−10 μL) to the pure water (demicellization of pure surfactant) or to the lipid vesicles (vesicles solubilization) in the calorimeter cell (capacity 1.335 mL) under constant stirring (∼400 rpm) conditions. The thermograms for each addition were recorded and analyzed using the supplied ORIGIN 5.0 software.

DSC Measurements. DSC measurements for the lipid−surfactant mixture were performed using a Microcal VP-DSC differential scanning calorimeter (Microcal, Inc., Northampton, MA). A temperature scan rate of 1 °C/min for both heating and cooling was used and the measurements were performed in the temperature interval from 25 to 90 °C. For a check of the reproducibility, three consecutive scans of each sample were recorded. The same software ORIGIN 5.0 was used for the evaluation of the experimental data.

Turbidity Measurements. Turbidimetric measurements of the lipid−surfactant mixtures were carried out using a Hewlett-Packard HP 8453 diode array spectrophotometer at a constant wavelength of 360 nm in the temperature scan mode. Absorbance was measured at 1 °C interval in the temperature range of 25−70 °C under constant stirring conditions (∼100 rpm) keeping the solution in a temperature controlled cell holder. The temperature of the cell was controlled by a Peltier system with a constant heating/cooling rate of 1 °C/min. The temperature equilibration time was 2 min for each measurement.

DLS Measurements. Dynamic light scattering experiments were performed with an ALV−NIBS high performance particle sizer equipped with a HeNe laser with 3 mW output power at a wavelength of 632.8 nm and an avalanche photodiode as detection system (ALV, Langen, Germany). The ALV−NIBS DLS instrument uses a backscattering arrangement, the scattering angle being 173°. With this instrument, a standard 1 cm quartz cells can be used. The temperature of the cell in the sample compartment was controlled by a Peltier temperature control unit. Data were analyzed using the supplied ALV−NIBS software which is based on the CONTIN software package using Laplace transforms for the inversion of the autocorrelation function. In the heating and cooling scans, the temperature was changed by one degree, and at each temperature, 3−5 measurements of 120 s duration of the autocorrelation function were performed. The time for one total heating−cooling cycle between 25 and 55 °C was between 6 and 10 h.

Results and Discussion

Isothermal Titration Calorimetry. The solubilization of DMPC vesicles by addition of surfactant was performed for each surfactant following the methods described earlier.[17−20] The experiments were performed at 30 and 60 °C and at different total lipid concentration in the cell. The concentration of surfactant in the syringe was chosen high enough to ensure complete solubilization of the vesicles after injection of the total syringe volume. The phase diagram for the surfactant-induced vesicle to micelle transition was obtained from the break points in the titration curves following the method described before.[20,23]

As an example for the solubilization experiment, we present two typical titration curves (Figure 2) obtained from the addition of a 130 mM micellar solution of SDS to DMPC vesicles at 30 and 60 °C together with the corresponding molar titration heat data and the differentiated curve to determine the D_t^{sat} and D_t^{sol} values. In the solubilization experiments, the first heats of injection are caused by the heat of demicellization of the surfactant plus the heat of incorporation of the surfactant into

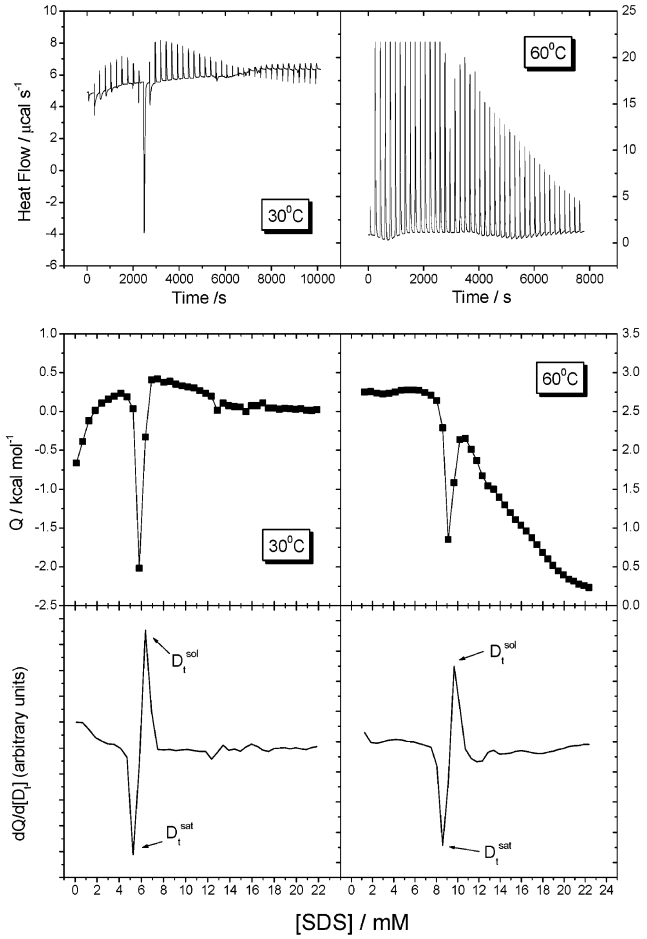

Figure 2. Titration of 247 μL of SDS solution (130 mM) into DMPC vesicles (2 mM) in 42 steps at 30 and 60 °C. Top: calorimetric traces (heat flow against time);'. Middle: reaction enthalpy versus [SDS] in the cell. Bottom: first derivative of the reaction enthalpy curve to determine the D_t^{sat} and D_t^{sol} values from the peaks.

the lipid bilayers. The latter contribution depends on the partition coefficient of the surfactant between water and bilayer. These processes continue until the vesicles are saturated with surfactant and the first mixed micelles appear. This is the region where the "dip" in the titration curves occurs. The heat effects beyond the "dip" are caused by heats of mixing of pure surfactant in micellar form with mixed micelles containing lipid.

For the construction of the phase diagram, measurements were performed at different lipid concentrations and also at different temperatures. For comparison, we also repeated the ITC experiment on the demicellization of surfactant in water following the earlier procedures.[27,28] The solubilization curves of DMPC vesicles with SDS in water along with heats of demicellization of SDS in water at 30 and 60 °C are presented in Figure 3. Detailed explanations of this type of solubilization curve are given in our previous publications.[20,23,27,28]

From the curves, it can be seen that at higher temperature more surfactant is required for the saturation of lipid vesicles with surfactant and for the solubilization of the vesicles. The transfer enthalpy of surfactant from micelles to bilayers becomes more endothermic with an increase in temperature. The D_t^{sat} and D_t^{sol} values are obtained from the first derivative of the curves and are plotted against total lipid concentration to construct the phase boundary lines (Figure 4) of the vesicle to micelle transition. It is observed that with an increase in temperature the phase boundary lines between the vesicular and micellar region are shifted to higher concentration indicating

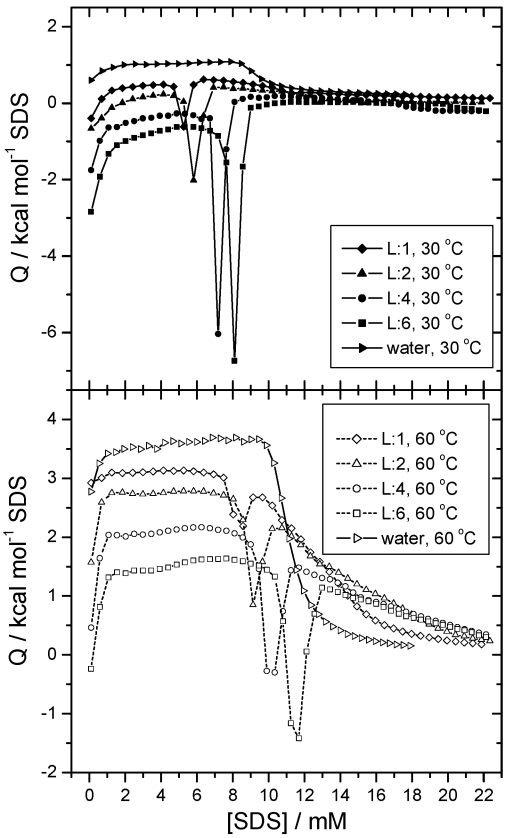

Figure 3. Reaction enthalpy Q versus total surfactant concentration in the cell for the titration of an SDS solution to DMPC vesicles at 30 and 60 °C with different DMPC concentrations. Reaction enthalpies for SDS demicellization in water are also given for a comparison. L: DMPC concentration in mM.

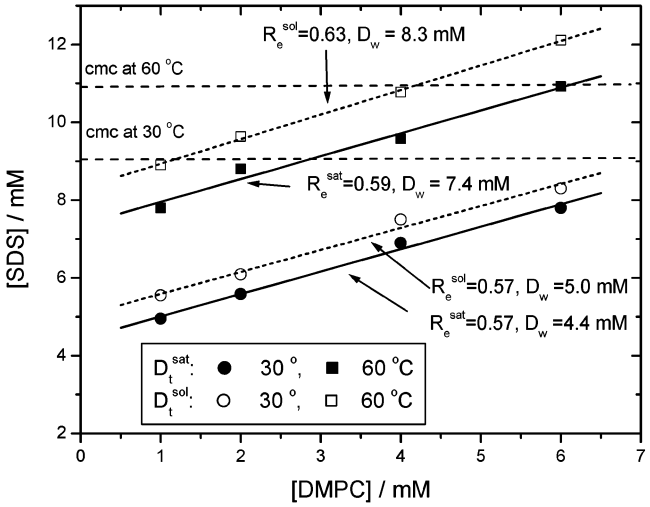

Figure 4. Phase diagram for DMPC−SDS−water at two different temperatures. The R_e^{sat} and R_e^{sol} values were calculated using a linear fit for the experimental data.

reduced partitioning of SDS into the bilayers at higher temperature, i.e., an increase in the water solubility of SDS characterized by an increase in the $D_w^{\#}$ values.

We have observed before with other negatively charged surfactants, such as cholate and deoxycholate, that the slopes of the coexistence lines, i.e., the R_e^{sat} and R_e^{sol} values, are almost the same when the solubilization of the vesicles is performed in water without additional salt.[23] This is also seen again in this study when SDS is used. For instance, whereas the R_e^{sat}

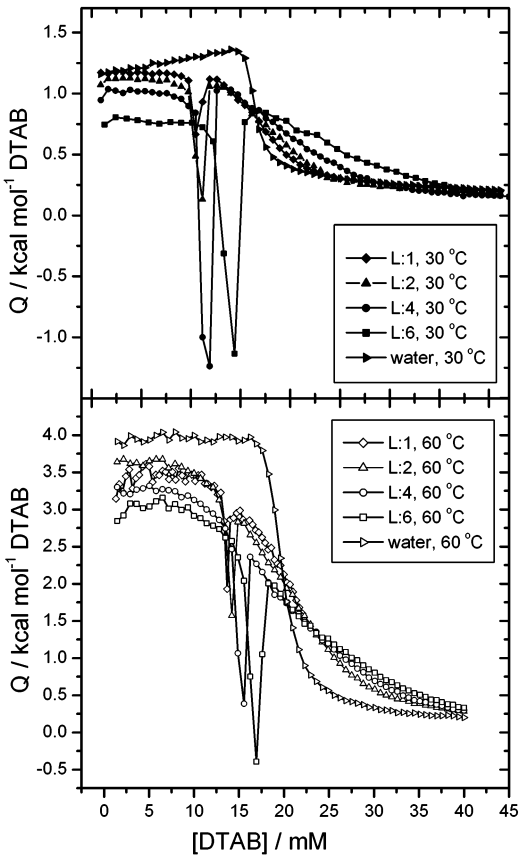

Figure 5. Reaction enthalpy Q versus total surfactant concentration in the cell for the titration of an DTAB solution into lipid vesicle at 30 and 60 °C and different DMPC concentrations. Reaction enthalpies for DTAB demicellization in water are also given for a comparison.

and R_e^{sol} values for the DMPC solubilization in water at 60 °C are 0.59 and 0.63, respectively (see Figure 4), they are much higher in 0.1 M NaCl and also the difference is much larger, namely, R_e^{sat} and R_e^{sol} are 1.05 and 1.52 (Majhi and Blume, unpublished).

The slopes of the coexistence lines are only slightly changed when the temperature is increased; that is, the vesicles become unstable at almost the same surfactant-to-lipid ratio. The only significant change is a slight increase in width of the coexistence region of mixed micelles and mixed vesicles at higher temperature of the phase boundaries at low lipid concentration as seen in Figure 4.

Compared to the solubilization of DMPC by octylglucoside,[20] much less surfactant is needed to saturate the bilayers as the lower R_e^{sat} values indicate. However, compared to the solubilization by cholates or deoxycholates, SDS is less effective, because the R_e^{sat} values of cholate and deoxycholate are much lower, namely, 0.11 and 0.19, respectively.[23]

Similar solubilization experiments were also performed with DMPC and the cationic surfactant DTAB. The results of the solubilization curves of DMPC with the cationic surfactant DTAB in water are shown in Figure 5.

Figure 6 shows the resulting phase diagram. This diagram is definitely different from all diagrams observed before so far, in that the D_t^{sat} and D_t^{sol} values show an upward curvature with increasing lipid concentration. The cause of this upward curvature is unclear at the moment. It means that with increasing lipid concentration the saturation concentration needed to render a vesicle unstable toward transformation into a mixed micelle increases. The R_e^{sat} values at low lipid concentration change

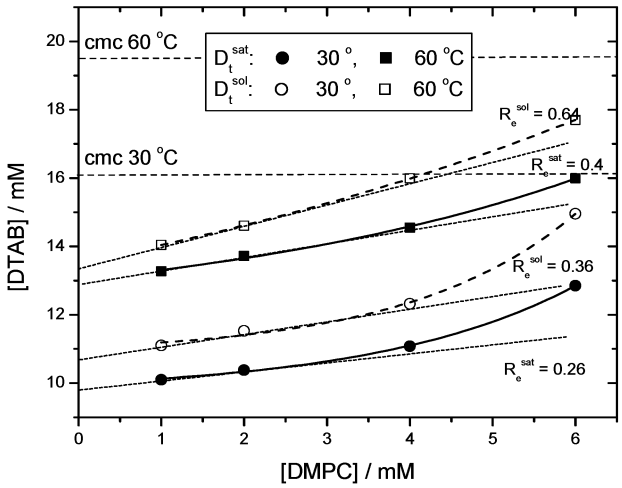

Figure 6. Phase diagram for DMPC-DTAB-water at two different temperatures with R_e^{sat} and R_e^{sol} values calculated from the slopes at low lipid concentration. The solid lines follow the experimental points and indicate higher $R_e^{\#}$ values at higher lipid concentration.

from ca. 0.26 to 0.4 at higher temperature. Overall, they are very similar to those observed for the anionic surfactant SDS and become only larger at higher lipid concentration. They also increase with temperature in a similar way.

From the phase diagrams obtained by ITC shown in Figures 4 and 6, we now constructed phase diagrams in the total surfactant concentration vs temperature plane with the total lipid concentration as a parameter (Figure 7). The phase boundary lines in this diagram were assumed in a first approximation to be described by a second-order polynomial similar to the temperature dependence of the cmc of surfactants with a minimum for the D_t^{sat} and D_t^{sol} values at the same temperature where the cmc minimum for SDS occurs. This is roughly between 20 and 25 °C.[27,29] This approximation is not unreasonable as measurements on the solubilization of soy bean PC with octyl-glucoside (OG) have shown where we indeed observed a very similar temperature dependence for D_t^{sat} and D_t^{sol} as observed for the cmc of OG (Keller and Blume, unpublished results).

In the top diagram of Figure 7, we included the cmc data for SDS in water for a comparison.[29] It is evident that D_t^{sat} shows a larger temperature dependence than the cmc., irrespective of how the exact curvature of the lines is. This means that at room temperature the cmc for SDS is higher than the SDS concentration needed for complete solubilization of a 6 mM DMPC vesicle solution, whereas at temperatures higher than 60 °C, higher concentrations than the respective cmc at these temperatures are needed for solubilization. The curvature is an indication for the temperature dependence of the thermodynamic transfer functions, in this case the equilibrium constant for the formation of surfactant saturated bilayers. As is evident from Figure 4 for SDS, the monomer concentration in equilibrium with the saturated bilayers increases with temperature from 5.3 to 8.7 mM. The diagram shows that for a fixed lipid and surfactant concentration the micellar, the coexistence, and the vesicular region can be reached by changes in temperature as indicated by the horizontal lines in Figure 7. They cross the phase boundaries at different temperatures t_1 and t_2, depending on the lipid and the surfactant concentration.

Figure 8 shows in a schematic way a three-dimensional phase diagram. The two-phase region of mixed vesicles and mixed micelles is located between two surfaces separating the mixed micelle region on the top of the diagram from the mixed vesicle

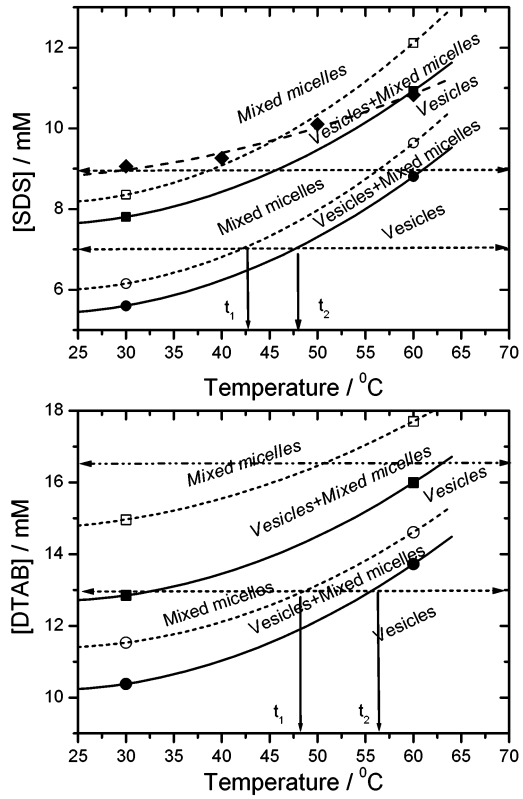

Figure 7. Phase diagram in the detergent concentration/temperature plane for two different DMPC concentrations. ●, ○, 2 mM DMPC; ■, □: 6 mM DMPC, − ◆ −. cmc of SDS in water.[29] Labeling in italics refers to the aggregate structures at 6 mM DMPC, and those in normal lettering refer to the system with 2 mM DMPC. The horizontal arrows refer to DSC experiments where at a fixed SDS or DTAB concentration and a given DMPC concentration the temperature was changed. For instance, for the 2 mM DMPC sample, the onset of vesiculation would be expected at $t_1 = 42.5$ °C for the system with SDS, and the micelle−vesicle transition should be complete at $t_2 = 48$ °C (top diagram).

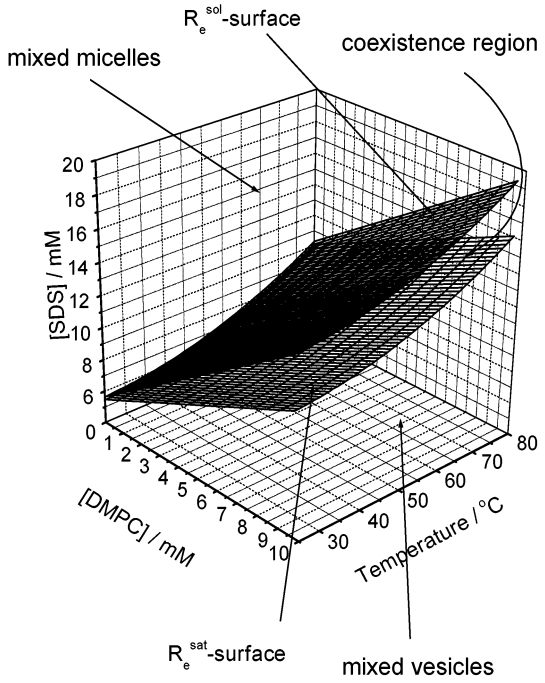

Figure 8. Schematic three-dimensional phase diagram for DMPC−SDS at high water concentration. The region between the two surfaces is the coexistence region of mixed micelles and mixed vesicles. This can be crossed in different ways at constant temperature by increasing the lipid or surfactant concentration or at fixed lipid and surfactant concentration by changing the temperature.

region in the lower part of the diagram at low surfactant concentration. It is evident from this diagram that the two phase region can be crossed either by going up vertically, i.e., increasing the surfactant concentration, or by going horizontally to higher temperature or higher lipid concentration.

UV−vis Turbidity Measurements. The transition from the micellar to the vesicular state should be observable using appropriate methods. The simplest way is to record the turbidity of the sample as a function of temperature. The formation of vesicles should lead to an increase in scattering intensity and likewise to an increase in turbidity with increasing temperature. To prove this assumption, we performed temperature-dependent turbidity measurements as shown in Figure 9 for DMPC/SDS and DMPC/DTAB.

It is evident that at a certain temperature, depending on the lipid and the surfactant concentration a large increase in turbidity is observed when the sample is heated. Upon further heating, the turbidity has an almost constant value till it increases again slightly up to a temperature of 70 °C. The cooling curves are definitely different from the heating curves. Cooling the samples starting at 70 °C first leads to a further slight increase in turbidity until the turbidity drops down again to very low values characteristic for micellar solutions. The observed turbidity changes are clearly caused by temperature induced micelle−vesicle transitions, i.e., a formation of vesicles upon heating and the break-down of vesicles into micelles upon cooling. The characteristic change in turbidity observed upon heating can be explained by comparing the temperature of the onset of turbidity increase and the end of the plateau region (Figure 9). When these temperatures are compared with the predicted temperature where the onset of vesicle formation should occur (see Figure 7) and where the coexistence region between micelles and vesicles should end, a relatively close agreement can be found. For instance, for the sample with 6 mM DMPC and 9 mM SDS, we would expect from Figure 7 that the coexistence range is between 39 and 47 °C. This agrees quite well with the temperature values taken from Figure 9, which are for the heating scan quite similar. Likewise, for the sample with 2 mM DMPC and 7 mM SDS, we would expect the coexistence range to extend from at least 43 to 49 °C (see arrows in Figure 7) which again agrees quite well with the values from the turbidity curve in Figure 9 (43 and 48 °C, respectively). For the DMPC-DTAB system, the agreement between the prediction taken from Figure 7 and turbidity curves shown in Figure 9 is much worse. For instance, for the sample with 2 mM DMPC and 13 mM DTAB, we would expect the coexistence range to extend from 48 to 57 °C. From Figure 9, we see that this is the range of the plateau region, but the initial increase in turbidity occurs at lower temperature. The poor agreement could be caused by slight variations in total surfactant concentration. As can be seen from Figure 7, the slopes of the lines delineating the coexistence region are relatively small. Therefore only slight variations in surfactant concentration can easily shift the onset of temperature induced vesiculation by several degrees.

The further increase in turbidity in the vesicular region is apparently caused by a change in size of the vesicles by aggregation and fusion. This would also explain the further increase in turbidity upon cooling before the coexistence region between micelles and vesicles is reached. In the cooling curves, the turbidity maximum occurs at a temperature where the coexistence region is entered and the first micelles are formed, and the temperature where the lowest absorbance value is reached agrees with the temperature where the micellar region

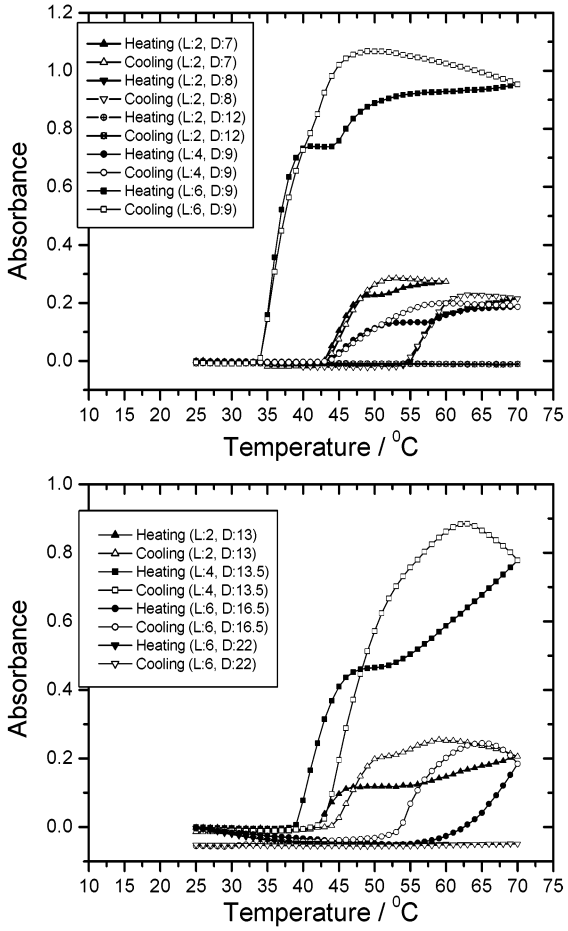

Figure 9. Turbidity at 360 nm of different DMPC−SDS mixtures (top) and DMPC−DTAB mixtures (bottom) as a function of temperature. The increase in turbidity at particular temperatures is caused by the formation of larger aggregates (vesicles). L: DMPC concentration in mM. D: surfactant concentration in mM.

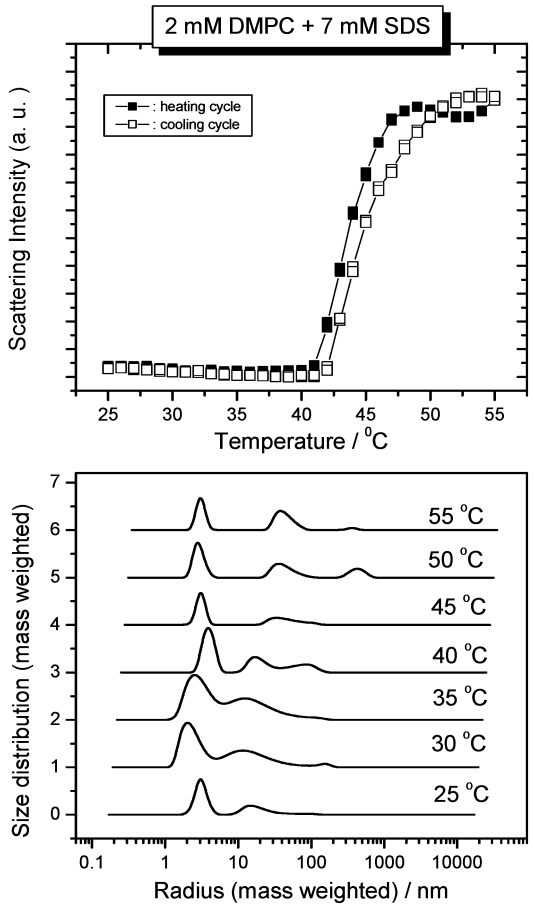

Figure 10. Top: Scattering intensity for a DMPC−SDS sample as a function of temperature as measured by DLS. Bottom: Mass-weighted size distribution for a DMPC−SDS sample in water as a function of temperature as measured by DLS (heating scan). The mass-weighted size distribution over-estimates the proportion of larger particles.

is entered. DMPC−DTAB mixtures show a characteristic difference in turbidity behavior in that the turbidity decrease observed upon cooling is in some cases observed at a higher temperature compared to the increase in turbidity seen upon heating the sample. The origin of this reversed hysteresis is unclear at present.

Dynamic Light Scattering. To check whether the increase in turbidity is really caused by the formation of vesicles, we also monitored the temperature induced micelle−vesicle transition by dynamic light scattering using the same experimental protocol. We measured the scattering intensity and size distribution as a function of temperature. It is seen from Figure 10 (top) for a DMPC/SDS sample that the scattering intensity changes in the same way as we observed in the turbidity measurements. Because of the limited temperature range of our DLS instrument, we could only extend the measurements to 55 °C. Therefore, we could not really reach the region where all micelles have disappeared and only vesicles exist. However, from the analysis of the particle size determined by dynamic light scattering, we could clearly see the change in relative composition in the mixed system with temperature. Figure 10 (bottom) shows the change of the mass-weighted distribution of particles as a function of temperature. At lower temperatures, mixed micelles with a hydrodynamic radius of ∼3 nm are present. However, also larger particles with a hydrodynamic radius of ∼10−20 nm can already be seen. These may correspond to elongated micelles. When the temperature is increased to values where the scattering intensity increases also dramatically, a new population of larger particles appears with an intermediate hydrodynamic radius of 30−40 nm. These particles could presumably be small vesicles. Above 45 °C, another population with radii in the range between 300 and 400 nm is formed. Probably larger vesicles are formed by fusion of the smaller ones. Even at the highest possible temperature of 55 °C attainable in our DLS instrument, a population of small micelles was still present, though its relative weight being reduced to 30−50 wt %, depending on the thermal history of the sample. As mentioned before, the micelle−vesicle transition is not yet complete at this particular temperature. The observed autocorrelation functions and the derived particle distributions varied when the temperature was held constant at 55 °C for several hours, but the general picture was always the same, namely, a smaller proportion of small particles with a radius of ∼3 nm and a higher proportion of larger particles with radii between 40 and 400 nm. It should be mentioned that the choice of a mass weighted distribution overemphasizes the larger particles. In reality, the percentage of lipid and surfactant in the larger aggregates is probably smaller.

The DLS measurements prove that the observed turbidity increase is indeed caused by a formation of vesicles, though the size distribution seems to be relatively broad. In addition, it seems as if with increasing temperature the average aggregate size increases.

In solubilization experiments with nonionic surfactants, usually a large increase in vesicle size by fusion of smaller vesicles is observed when the saturation limit is reached.[7,20,24−26] This is different for the solubilization of lipid vesicles by SDS

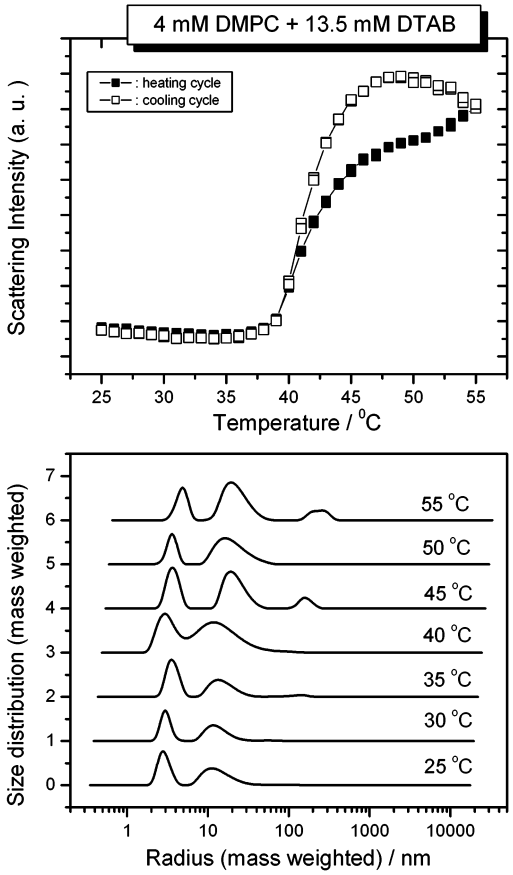

Figure 11. Top: Scattering intensity for a DMPC−DTAB sample as a function of temperature as measured by DLS. Bottom: Mass-weighted size distribution for a DMPC−DTAB sample in water as a function of temperature as measured by DLS (heating scan). The mass-weighted size distribution over-estimates the proportion of larger particles.

or DTAB where no size increase was observed up to D_t^{sat} as measured by DLS (results not shown). The reason for this different behavior is probably simply that the vesicles carry a negative charge which prevents vesicle growth by fusion. The size changes of the vesicles observed by temperature increase are therefore unexpected, since the vesicles are also negatively charged in this case. A possible explanation could be a temperature dependent decrease of the positive spontaneous curvature leading to a larger tendency for fusion. Additional preliminary experiments performed by reaching the high temperature in a short time yielded a different vesicle distribution than in the slow scan. Also, it was observed that after a fast temperature jump to 55 °C the vesicle distribution changed slightly with time in the first 10 min. Further experiments are clearly necessary to pursue this phenomenon particularly at higher temperatures which was not possible with our DLS equipment.

The DMPC−DTAB−water systems also show a similar size distribution pattern with temperature (see Figure 11). The difference for the DMPC−DTAB system is that at higher temperature, where the first vesicles appear, their size is somewhat smaller than for DMPC−SDS mixtures. At high temperature, an additional peak appears again in the size distribution, with the average radius of these particles being around 150−250 nm. At the highest temperature attainable in our DLS (55 °C), the percentage of larger particles (vesicles) has increased but the micelle−vesicle transition is not complete yet. From the "phase diagram" in Figure 8 and the turbidity curves in Figure 9, we would estimate that a temperature of at least 65 °C is necessary for a complete transformation into mixed vesicles.

Differential Scanning Calorimetry. The results obtained using turbidity and DLS measurements showed that indeed a temperature-induced micelle−vesicle transition takes place in DMPC−surfactant mixtures of defined composition. We now wondered whether these transitions can also be observed by differential scanning calorimetry. A prerequisite for such an event being observable by DSC is that this transition is connected with a heat effect. That this will occur is not a priori clear when the results of the ITC experiments are taken into account. From these experiments, it was clear that the transfer enthalpy of a surfactant from water to a micelle or to a bilayer vesicle is temperature dependent, but the magnitude of the transfer enthalpy into bilayers cannot easily determined from the present experiments unless the partition coefficient is known. The micellization enthalpies of SDS and DTAB, however, are well-known. In a transition from mixed micelles to mixed vesicles, also, a phospholipid is transferred between the two aggregates. This leads to two contributions to the observed heat effect, which cannot be separated. Our hope was that in the DSC curves this transition should be observable in the case that these heat effects would not compensate.

Our experimental protocol for the DSC measurements was essentially the same as that for the turbidity measurement. Samples with a specific composition, i.e., DMPC-to-surfactant ratio chosen in such a way that the systems were in a state of mixed micelles at room temperature, were filled into the sample cell of the calorimeter and heated to high temperature and cooled again.

Figure 12 shows the heating and cooling curves for several DMPC−SDS−water samples with lipid−surfactant compositions as indicated. It is obvious that in most curves definite deviations from the baseline are observed, which are different and more distinct in the cooling curves. For two sample compositions, i.e., 2 mM DMPC + 4 mM SDS and 6 mM DMPC + 6 mM SDS, only baselines are observed. This is due to the fact that for these compositions the aggregation state does not change with temperature. In this case, vesicles are present in the whole temperature range. In the third case, with 2 mM DMPC + 12 mM SDS, only mixed micelles are present in the whole temperature range, and the state of aggregation also does not change with temperature. In all other cases, the transition region between micelles and vesicles is crossed as already seen in the turbidity measurements and also concluded from the phase diagrams in Figures 7 and 8.

The increase in heat capacity below 30 °C observed in the cooling curves is probably caused by the liquid-crystalline to gel phase transition of the system. For DMPC, the transition temperature for the pure DMPC vesicles is located at 24 °C. For the mixed micellar system, the formation of gel phase bilayers with some incorporated surfactant is usually observed at a somewhat lower temperature upon cooling. The resulting structures at low temperature may be mixed micelles with a crystalline core as observed for DMPC with $C_{12}E_8$[13] or for the systems DMPC and DPPC with NaC.[11] In the latter study, DSC curves running to low temperature were reported and very large heat effects due to lipid chain melting were observed. We have not studied our systems in the region of the chain melting transition because we wanted to focus on the micelle-vesicle transition between "fluid" systems and want to emphasize again, that the vesicles formed upon heating are in the liquid-crystalline state and that the observed heat effects are solely due to nonzero

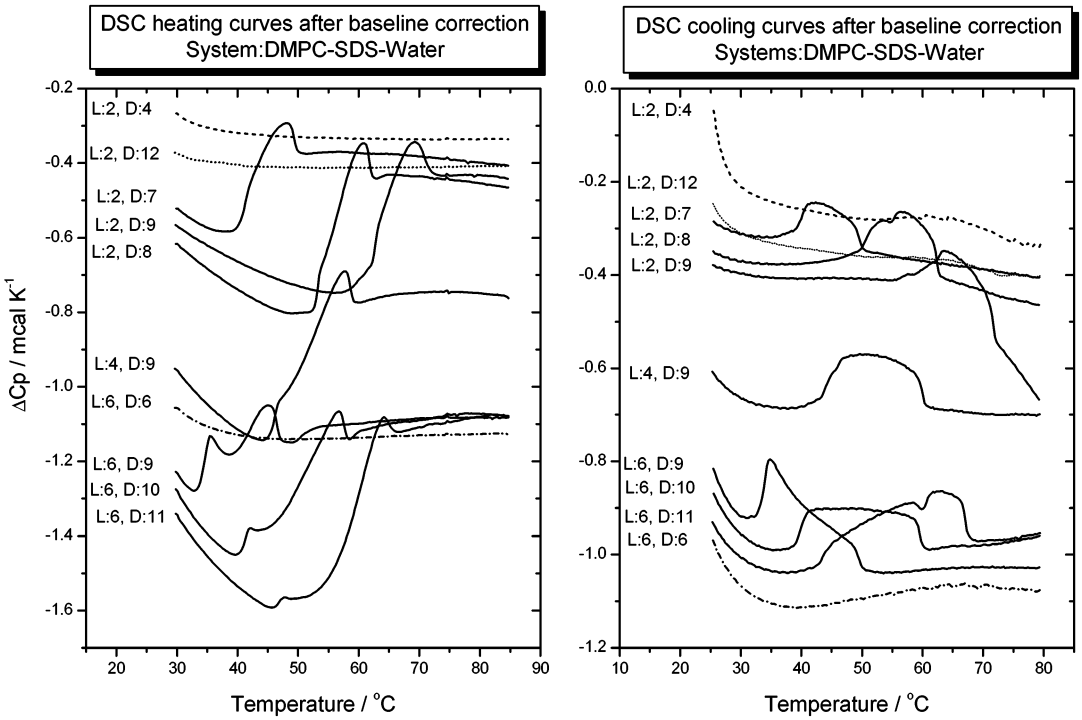

Figure 12. DSC heating (left) and cooling (right) curves for various DMPC−SDS samples. L = DMPC concentration in mM. D = SDS concentration in mM.

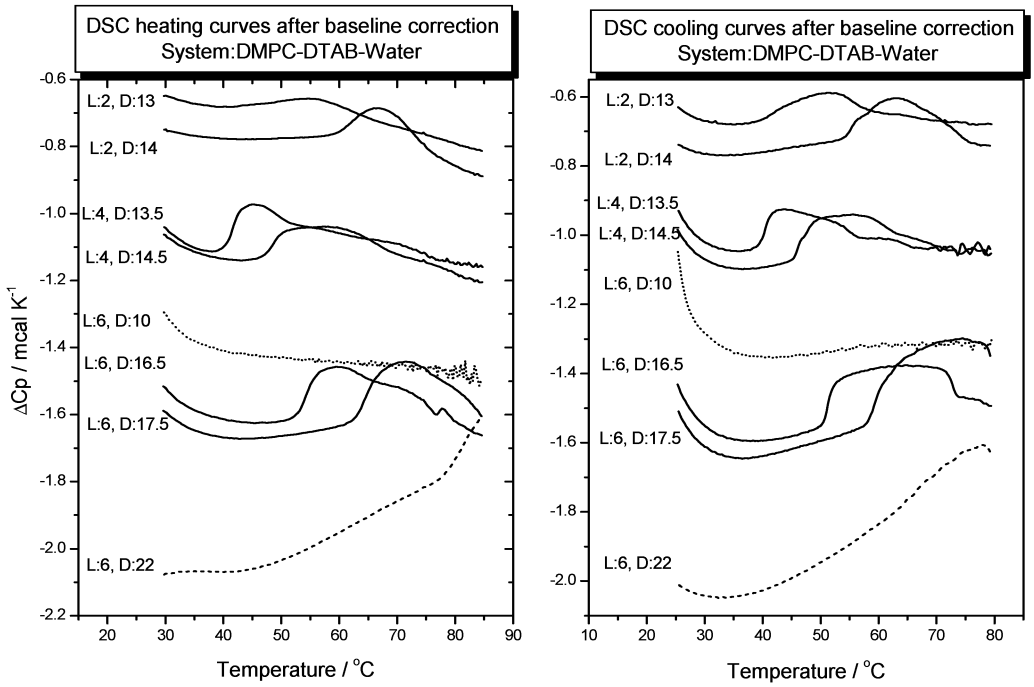

Figure 13. DSC heating (left) and cooling (right) curves for various DMPC−DTAB samples. L = DMPC concentration in mM. D = DTAB concentration in mM.

transfer enthalpies of surfactant and lipid between micelles and fluid vesicles (see below).

Figure 13 shows similar DSC curves for the system DMPC−DTAB−water. In this case also, endothermic effects can be observed upon heating and exothermic upon cooling. For DMPC−DTAB, however, the differences between the heating curves and the cooling curves are not so large as for the DMPC−SDS system shown in Figure 13. Again, the heat effects occur in a temperature range where the micelle−vesicle transition should be observed as judged from the turbidity curves and the phase diagrams in Figures 7 and 8.

We have analyzed the behavior of the DMPC−SDS system in some more detail and compared directly the DSC curves of two different DMPC−SDS samples with the turbidity curves obtained from the same samples (see Figure 14). It can be seen that the onset of the turbidity increase upon heating does not coincide with the peak onsets in the DSC curves but rather with the first step of the C_p increase in the DSC heating curve. Likewise upon cooling, at the temperature where the turbidity has already decreased to the lowest value, the C_p values in the DSC cooling curve have not decreased yet. It seems as if heat effects are already present before a significant increase in

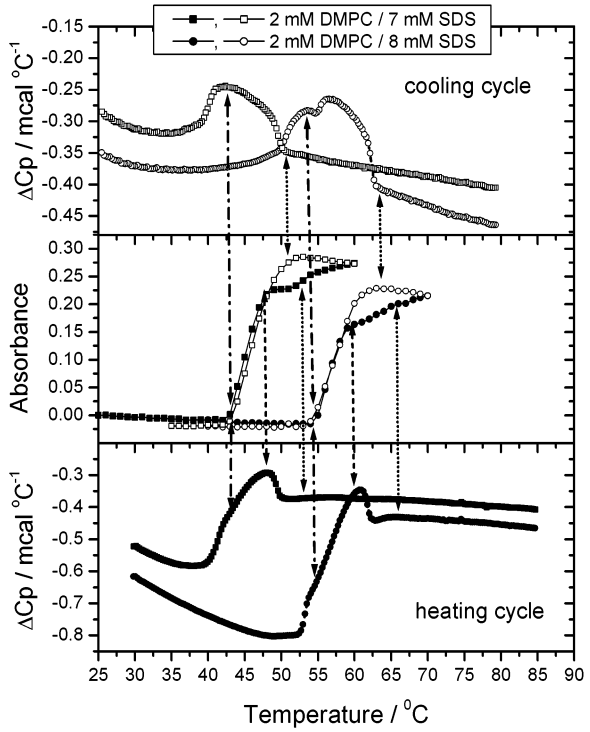

Figure 14. Top: DSC cooling curve. Bottom: DSC heating curve for two different DMPC−SDS samples. Middle: Turbidity vs temperature curves for the same sample preparation. The arrows point to the beginning of the turbidity increase, to the beginning and the end of the plateau region in the heating curve, respectively, and to the beginning and end of the turbidity decrease in the cooling curve, respectively.

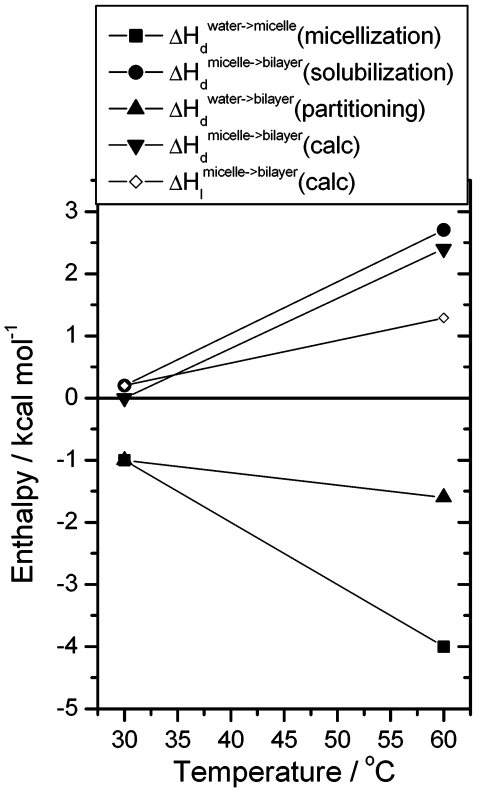

Figure 15. Transfer enthalpies for the surfactant SDS (*d*) and the lipid DMPC (*l*) between water or different types of aggregates at two different temperatures as determined from isothermal titration calorimetry.

turbidity is observed. These effects may be caused by the transformation of smaller mixed micelles to larger aggregates, i.e., elongated micelles or bilayers sheets or disks. As judged from the DLS curves, these types of aggregates are indeed already present at a lower temperature (see Figure 10).

The question now arises why we observe heat effects at all in the DSC curves although both types of aggregates, the mixed micelles and the mixed vesicles, are in a fluid state. As already proposed above, the heat effects must arise from the transfer of surfactant and lipid from mixed micelles to mixed vesicles. Both of these enthalpies must be positive to cause the endothermic effects. The transfer enthalpy for the detergent from micelles to vesicles $\Delta H_{\text{detergent}}^{\text{mic}\rightarrow\text{bilayer}}$ can be determined from the experimental solubilization curves or calculated from the difference in the transfer enthalpies of the detergent from water to micelle (micellization) and water to a bilayer (partitioning), respectively. For instance, the heat effects observed upon addition of a micellar SDS solution to a DMPC vesicle suspension in the region below solubilization of the vesicles is in a first approximation when the monomer concentration of SDS is neglected directly the transfer enthalpy of SDS from micelles to vesicles $\Delta H_{\text{detergent}}^{\text{mic}\rightarrow\text{bilayer}}$. From Figure 3, we can see that for a 2 mM DMPC vesicle suspension the values are ∼0.2 and ∼2.7 kcal mol^{-1} at 30 and 60 °C, respectively. Similar values can be calculated from the differences of the partitioning enthalpy $\Delta H_{\text{detergent}}^{\text{mic}\rightarrow\text{bilayer}}$, determined in a separate experiment (not shown), and the micellization enthalpy $\Delta H_{\text{detergent}}^{\text{water}\rightarrow\text{micelle}}$ at 30 (−1 kcal mol^{-1}) and 60 °C (−4 kcal mol^{-1}) determined from the demicellization curves in Figure 3.

The transfer enthalpy $\Delta H_{\text{lipid}}^{\text{mic}\rightarrow\text{bilayer}}$ for the lipid from the mixed micelle to the bilayer can also be estimated from the titration curves in Figure 3 from the heat observed in the "dip region", i.e., the coexistence range of mixed micelles and mixed vesicles. For the solubilization experiments, we have shown that this is related to the transfer enthalpies using the following expression:[18]

$$\Delta H = -\frac{x_{sat}(1-x_{sol})}{x_{sol}-x_{sat}}\Delta H_{\text{detergent}}^{\text{mic}\rightarrow\text{bil}} + \frac{(1-x_{sol})(1-x_{sat})}{x_{sol}-x_{sat}}\Delta H_{\text{lipid}}^{\text{bil}\rightarrow\text{micelle}} + \Delta H_{\text{detergent}}^{\text{mic}\rightarrow\text{mixmic}}$$

with

$$x_{\text{sat}} = \frac{R_{\text{e}}^{\text{sat}}}{1+R_{\text{e}}^{\text{sat}}}$$

and

$$x_{\text{sol}} = \frac{R_{\text{e}}^{\text{sol}}}{1+R_{\text{e}}^{\text{sol}}}$$

This equation was originally derived assuming a negligible monomer surfactant concentration but is also valid with the approximation that in the coexistence region the monomer concentration remains constant. Assuming additionally that the third term, the mixing enthalpy of pure and mixed micelles, is negligible, we can determine $\Delta H_{\text{lipid}}^{\text{mic}\rightarrow\text{bilayer}}$ from the experimental curves knowing the values for x_{sat}, x_{sol} (see Figure 4), and the transfer enthalpy $\Delta H_{\text{detergent}}^{\text{mic}\rightarrow\text{bilayer}}$ (see above).

Figure 15 shows the measured and calculated values at 30 and 60 °C. From the graph, it is clear that the transfer enthalpy $\Delta H_{\text{detergent}}^{\text{mic}\rightarrow\text{bilayer}}$ is almost zero at 30 °C and increases strongly with temperature, whereas $\Delta H_{\text{lipid}}^{\text{mic}\rightarrow\text{bilayer}}$ is positive at both

temperatures and increases also with temperature but to a smaller extent. Because both species, the detergent and the lipid, are transferred from micelles to bilayers with increasing temperature, an endothermic effect is the result, as experimentally observed in the DSC experiment. The increase in $\Delta H_{\text{detergent}}^{\text{mic}\rightarrow\text{bilayer}}$ with temperature can be discussed on the basis of the thermodynamics observed for the hydrophobic effect. Negative ΔC_p values are normally observed for the transfer enthalpies of hydrophobic molecules from water to a hydrocarbon environment. They are proportional to the shielding of hydrophobic surfaces from water in a hydrocarbon solvent or the inner core of a micelle or a bilayer.[20,27] This is the reason for the decrease in micellization enthalpy at higher temperature (see Figure 15). The increase in $\Delta H_{\text{detergent}}^{\text{mic}\rightarrow\text{bilayer}}$ observed here would mean that at higher temperature the surfactant SDS in a mixed micelle is better shielded from water than in a mixed vesicle. This is easily interpreted in terms of a structural model. For the lipid DMPC, a smaller difference exists in the transfer enthalpy $\Delta H_{\text{lipid}}^{\text{mic}\rightarrow\text{bilayer}}$ between 30 and 60 °C. However, the ΔC_p value is also positive meaning a better shielding of the hydrocarbon surfaces of DMPC in a micelle compared to a vesicle. However, this interpretation has to be viewed with caution, because only contributions from hydrophobic hydration are taken into consideration for the explanation of the positive ΔC_p values.

For the transfer of octylglucoside at 28 °C, values for $\Delta H_{\text{detergent}}^{\text{mic}\rightarrow\text{bilayer}} = 645$ cal mol^{-1} and for $\Delta H_{\text{lipid}}^{\text{mic}\rightarrow\text{bilayer}} = -592$ cal mol^{-1} were reported by Opatowski at al.[30] Compared to our values for SDS and DMPC, the major difference is the change in sign for $\Delta H_{\text{lipid}}^{\text{mic}\rightarrow\text{bilayer}}$ for the transfer of DMPC from mixed micelles to mixed bilayers. A straightforward explanation is difficult because ionic surfactants behave differently compared to nonionic. In addition, Opatowski et al.[30] reported no values at higher temperature so that a comparison of the temperature dependence of the transfer enthalpy of the lipid cannot be made. It might well be that at higher temperature $\Delta H_{\text{lipid}}^{\text{mic}\rightarrow\text{bilayer}}$ for octylglucoside is also positive.

A different approach to understand the observed DSC curves is to take the experimental ITC curves (Figure 3) and calculate from these data the enthalpy of the system at a particular lipid and detergent concentration and at different temperatures. Because we have only experimental curves at 30 and 60 °C, we constructed some interpolated curves for the solubilization experiment as shown in Figure 16 (top). The interpolation was performed by assuming a linear dependence of the observed titration heats with temperature. This is justified, because other measurements with more experimental temperature performed on the system DMPG/octylglucoside showed just this behavior (Keller and Blume, unpublished). From the experimental and interpolated ITC solubilization curves, the integrated enthalpy as a function of SDS concentration was then calculated, for instance, for a sample with a concentration of 2 mM DMPC in 1.334 mL volume as shown on the bottom of Figure 16.

The "dip" in the heat effects observed in the coexistence region of mixed micelles and mixed vesicles (top of Figure 16) is smeared out and less obvious in the integrated curve at the bottom. However, it is still quite obvious that the vertical arrow drawn at a fixed concentration of 7 mM SDS crosses the experimental and interpolated curves on the right-hand side of this dip at lower temperature and the left-hand side at higher temperature, meaning that the system goes from a micellar state at low to a vesicular state at high temperature.

From this diagram, the enthalpy for a 0.512 mL sample (volume of the DSC cell) of 2 mM DMPC and 7 mM SDS as a function of temperature was constructed as shown in Figure 17 (top). In a DSC experiment, the change in enthalpy with temperature is recorded. Therefore, the differentiated curve on the bottom of Figure 17 has to be considered. It corresponds to the heat capacity of the system and its change with temperature. It can be seen that the curve calculated for the DMPC−SDS sample resembles the experimental curve for a sample of the same composition (see Figure 13), particularly when the total change in C_p is considered.

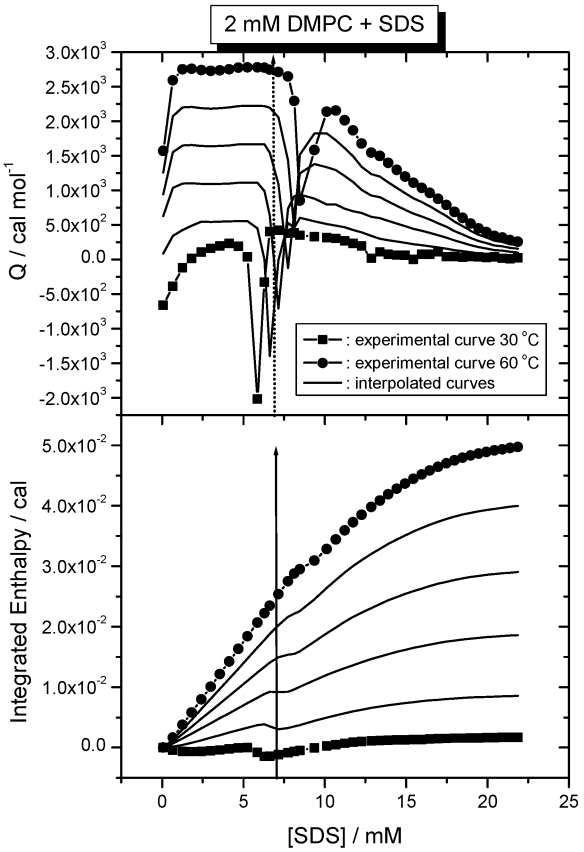

Figure 16. Top: Experimental and interpolated ITC solubilization curves for 2 mM DMPC with SDS. Bottom: Integrated curves giving the enthalpy of the surfactant as a function of SDS concentration in the cell (1.334 mL). The vertical arrow corresponds to a change in the enthalpy with temperature at a fixed SDS concentration.

The details of the calculated C_p curve are different. This is not surprising because of our crude interpolation method of the experimental ITC curves. However, Figures 16 and 17 show that the results of the ITC experiments are consistent with the DSC results and that, in principle, if ITC experiments at many more temperatures would have been performed, the DSC curves could have more precisely been calculated from the ITC experiments.

Summary and Conclusions

The temperature-induced micelle−vesicle transition in mixed phospholipid−surfactant systems can be understood on the basis of experimental results using isothermal titration calorimetry. From these results, a three-dimensional phase diagram can be constructed which shows that not only concentration-induced changes in aggregation state are possible but also temperature can be used as a parameter to cross the coexistence region of mixed micelles and mixed vesicles. The reason for this behavior is the fact that the surfaces enclosing the coexistence regions of mixed micelles and mixed vesicles in a lipid−surfactant mixture are curved in the direction of the temperature axis

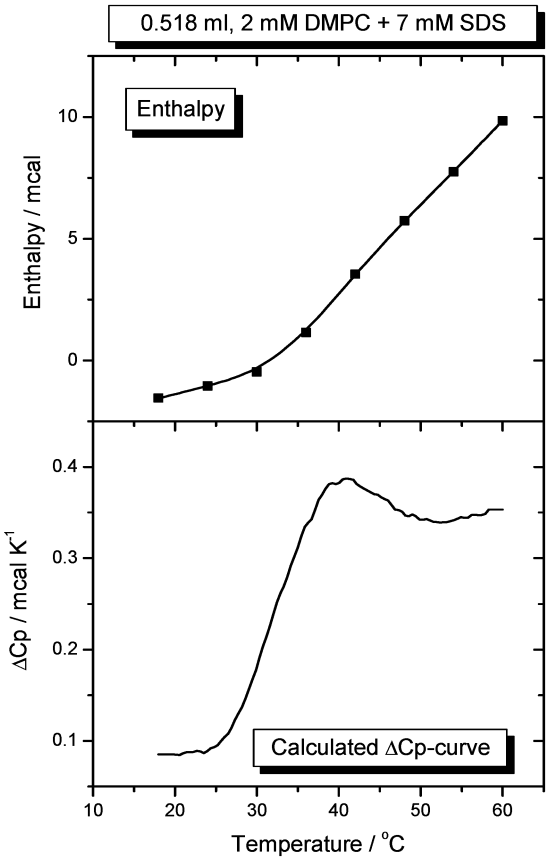

Figure 17. Top: Enthalpy of SDS as a function of temperature for a sample of 0.512 mL of 2 mM DMPC and 7 mM SDS as calculated from Figure 16 (bottom). Bottom: differentiated curve of the enthalpy giving the heat capacity of SDS as a function of temperature.

because of the temperature dependence of the hydrophobic effect. The temperature dependence of the surfactant concentration need for saturation and solubilization of lipid vesicles shows a similar temperature dependence as the cmc of the surfactant; that is, these concentrations increase with increasing temperature above a certain temperature where they are minimal. In the simple binary system surfactant−water, this leads to the phenomenon that in a surfactant solution with a concentration just above the minimal cmc at higher temperature a demicellization is observed; that is, the monomer state is preferred.[29] In the ternary system phospholipid−surfactant−water, the larger aggregate, the vesicle, is more stable than the mixed micelle. This result is the consequence of the temperature dependence of the saturation and solubilization concentrations but is not easy to understand, and it seems at a first glance paradoxical that above a certain temperature the vesicular aggregates are more stable than micelles, because vesicles are usually thought of as a state of aggregation with higher order. However, the phenomenon can be understood on the basis of the thermodynamic state functions, though this gives no obvious interpretation in terms of structure. The positive temperature dependence of the transfer enthalpy for a surfactant from a micelle to a vesicle can be interpreted on the basis of the hydrophobic effect but is also not easily understood in terms of structural differences between the bilayer and the micelle. It is possible that electrostatic effects play an important role, because we could not observe clear transitions in the DSC curves of phospholipids with nonionic surfactants such as octyl-glucoside or decyl-maltoside, though the turbidity curves indicated the formation of larger aggregates at higher temperature. These findings have to be clarified in future experiments.

The results presented here clearly show that a temperature increase can be utilized to induce vesicle formation from mixed micelles. The reverse process, namely, the "solubilization" of vesicles, i.e., the transformation of vesicles saturated with surfactant by a temperature decrease, is also possible. This offers new possibilities in systems with biological membranes, namely, a solubilization procedure of detergent saturated membranes by cooling or reconstitution of proteins into bilayers by mild warming at constant surfactant concentration.

Acknowledgment. This work was supported by grants from the Deutsche Forschungsgemeinschaft and the Fonds der Chemischen Industrie.

References and Notes

(1) Almong, S.; Kushnir, T.; Nir, S.; Lichtenberg, D. *Biochemistry* **1986**, *25*, 2597.

(2) Schurtenberger, P.; Mazer, N. A.; Kanzig, W. *J. Phys. Chem.* **1985**, *89*, 1042.

(3) Aveldano, M. I. *Arch. Biochem. Biophys* **1995**, *324*, 331.

(4) Jiang, S. S.; Fan, L. L.; Yang, S. J.; Kuo, S. Y.; Pan, R. L. *Arch. Biochem. Biophys.* **1997**, *346*, 105.

(5) Inoue, T. Interaction of Surfactant with Phospholipid Vesicles. In *Vesicles*; Rosoff, M., Ed.; Marcel Dekker Inc.: New York, 1996; Surfactant Science Series, Volume 62, Chapter 5.

(6) Wenk, M. R.; Alt, T.; Seelig, J. *Biophys. J.* **1997**, *72*, 1719.

(7) Lichtenberg, D. Liposomes as a Model for Solubilization and Reconstitution of Membranes. In *Handbook of Nonmedical Applications of Liposomes*; Lasic, D. D., Barenholz, Y., Eds.; CRC Press: Boca Roton, FL, 1996; Vol. II, Chapter 3.

(8) Lasic, D. D. In *Liposomes: from Physics to Applications*; Elsevier Scieence Publishers: Amsterdam, 1993.

(9) Helenius, A.; Simons, K. *Biochim. Biophys. Acta*. **1975**, *29*, 415.

(10) Urbaneja, M. A.; Alonso, A.; Gonzalez-Manas, J. M.; Goni, F. M.; Partearroyo, M. A.; Tribout, M.; Paredes, S. *Biochem. J.* **1990**, *270*, 305.

(11) Polozova, A. L.; Dubachev, G. E.; Simonova, T. N.; Barsukov, L. I. *FEBS Lett.* **1995**, *358*, 17.

(12) Lesieur, P.; Kiselev, M. A.; Barsukov, L. I.; Lombardo, D. *J. Appl. Cryst.* **2000**, *33*, 623.

(13) Funari, S. S.; Nuscher, B.; Rapp, G.; Beyer, K. *Proc. Natl. Acad. Sci. U.S.A.* **2001**, *98*, 8938.

(14) Otten, D.; Lobbecke, L.; Beyer, K. *Biophys. J.* **1995**, *68*, 584.

(15) Forte, L.; Andrieux, K.; Keller, G.; Grabielle-Madelmont, C.; Lesieur, S.; Paternostre, M.; Ollivon, M.; Bougaux, C.; Lesieur, P. *J. Therm. Anal.* **1998**, *51*, 773.

(16) Lasch, J. *Biochim. Biophys. Acta* **1995**, *1241*, 269.

(17) Heerklotz, H.; Lantzsch, G.; Binder, H.; Klose, G.; Blume, A. *Chem. Phys. Lett.* **1995**, *235*, 537.

(18) Heerklotz, H.; Lantzsch, G.; Binder, H.; Klose, G.; Blume, A. *J. Phys. Chem.* **1996**, *100*, 6764.

(19) Heerklotz, H.; Lantzsch, G.; Binder, H.; Klose, G.; Blume, A. *J. Phys. Chem.* **1997**, *101*, 639.

(20) Keller, M.; Kerth, A.; Blume, A. *Biochim. Biophys. Acta* **1997**, *1326*, 178.

(21) Wenk, M. R.; Seelig, J. *Biophys. J.* **1997**, *73*, 2565.

(22) Opatowski, E.; Kozlov, M. M.; Lichtenberg, D. *Biophys. J.* **1997**, *73*, 1448.

(23) Hildebrand, A.; Garidel, P.; Neubert, R.; Blume, A. *Langmuir* **2002**, *18*, 2836

(24) Lichtenberg, D. *Biochim. Biophys. Acta* **1985**, *821*, 470.

(25) Lichtenberg, D.; Opatowski, E.; Kozlov, M. M. *Biochim. Biophys. Acta* **2000**, *1508*, 1.

(26) Lichtenberg, D. In *Biomembranes: Physical Aspects*; Shinitzky, M., Ed.; VCH: Weinheim, Germany, 1993; pp 63−95.

(27) Paula, S.; Sues, W.; Tuchtenhagen, J.; Blume, A. *J. Phys. Chem.* **1995**, *99*, 11742.

(28) Majhi, P. R.; Moulik, S. P. *Langmuir* **1998**, *14*, 3986.

(29) Majhi, P. R.; Blume, A. *Langmuir* **2001**, *17*, 3844.

(30) Opatowski, E.; Lichtenberg, D.; Kozlov, M. M. *Biophys. J.* **1997**, *73*, 1458.